

KeyframeFace: From Text to Expressive Facial Keyframes

Jingchao Wu^{1,2*} Zejian Kang^{3,1*} Haibo Liu¹ Yuanchen Fei^{1,4} Xiangru Huang^{1†}

¹ Westlake University

² Nanjing University

³ Zhejiang University

⁴ Hunan University

jcwu@smail.nju.edu.cn huangxiangru@westlake.edu.cn



Figure 1: **Our text-to-animation model enabled by the KeyframeFace dataset.** Given descriptions of contextual background and desired emotions, our text-to-animation framework produces keyframe-level facial descriptions and generates the corresponding ARKit coefficients that can be directly converted into expressive facial animations and videos via tools like MetaHuman.

Abstract

Generating dynamic 3D facial animation from natural language requires understanding both temporally structured semantics and fine-grained expression changes. Existing datasets and methods mainly focus on speech-driven animation or unstructured expression sequences and therefore lack the semantic grounding and temporal structures needed for expressive human performance generation. In this work, we introduce **KeyframeFace**, a large-scale multimodal dataset designed for text-to-animation research through keyframe-level supervision. KeyframeFace provides 2,100 expressive scripts paired with monocular videos, per-frame ARKit coefficients, contextual backgrounds, complex emotions, manually defined keyframes, and multi-perspective annotations based on ARKit coefficients and images via Large Language Models (LLMs)/Multimodal Large Language Models (MLLMs). Beyond the dataset, we propose **the first text-**

to-animation framework that explicitly leverages LLM priors for interpretable facial motion synthesis. This design aligns the semantic understanding capabilities of LLMs with the interpretable structure of ARKit’s coefficients, enabling high-fidelity expressive animation. KeyframeFace and our LLM-based framework together establish a new foundation for interpretable, keyframe-guided, and context-aware text-to-animation. Code and data are available at <https://github.com/wjc12345123/KeyframeFace>.

1 Introduction

Generating 3D dynamic facial animation from natural-language description is a long-standing goal in computer vision and graphics, enabling human-computer interaction, virtual reality, digital humans, and emotion-aware avatars. Existing studies mainly focus on either speech-driven talking

* Equal contribution. † Corresponding author: huangxiangru@westlake.edu.cn

faces [12, 24] or generation [6, 48], but they often fail to capture the fine-grained temporal structures and contextual reasoning that are crucial for expressive human performance generation.

In this paper, we argue that human expressions are not isolated actions — they evolve through key expressive moments guided by situational background and emotional intent. Expressive human performance can comprise rapid and subtle muscular or emotional transitions that should be modeled with structured semantics and anatomically-accurate facial muscle movements — or its practical approximations, such as FACS [11] or ARKit-based blendshape [10] coefficients.

To address these challenges, we propose **Keyframe-Face** that establishes a unified framework for text-to-facial-animation generation through keyframe-level semantic supervision. KeyframeFace is a large-scale and richly-annotated multimodal dataset containing **2,100** expressive scripts, each enacted by human actors and recorded with cellphone devices. The recorded monocular videos are annotated with contextual background, complex or composite emotions, and manually defined facial keyframes. Each keyframe is aligned with both ARKit-based blendshape coefficients and detailed textual descriptions, forming a rich set of text-motion correspondences.

Beyond constructing the dataset, we introduce the first LLM-driven text-to-animation framework that explicitly leverages semantic priors of large language models. This design not only aligns natural language with interpretable facial controls but also enables controllable and context-aware animation synthesis without relying on categorical emotion labels.

Extensive experiments demonstrate that semantic supervision—particularly the combination of LLM-driven keyframe descriptions and ARKit-based annotations—significantly improves expression fidelity, text-motion alignment, and temporal coherence compared to non-semantic baselines.

Our main contributions are summarized as follows:

- We construct KeyframeFace dataset, the first multimodal corpus featuring contextual background, complex emotional transitions, and keyframe-level descriptions aligned with ARKit-based blendshapes.
- We introduce the first LLM-driven text-to-animation framework that explicitly leverages semantic priors of large language models.

2 Related Work

Temporal Structure Modeling In Video Generation. Recent advances in video generation have explored various temporal modeling strategies. Frame-level autoregressive models [14, 9, 29, 33, 7] extend language modeling to the temporal domain but face high computational cost and weak long-term consistency. Multi-track timeline control methods [47, 17, 22, 3, 5] achieve precise temporal scheduling, but they typically require

complex user interaction and dense temporal annotations, limiting scalability and generalization in real-world applications. Keyframe-based approaches [40, 21, 38, 12, 4, 19, 35] show strong potential by efficiently capturing the core temporal structure of videos and accurately representing fine-grained details at critical moments. In particular, keyframe-driven facial animation methods [12, 4, 19, 35] identify expressive key moments to generate primary facial frames and interpolate intermediate frames, reducing cross-modal mapping uncertainty and improving temporal coherence and controllability. Despite remarkable progress, most existing keyframe-based methods are often modality-specific and lack a unified framework for direct text-to-3D keyframe generation. In this paper, we propose a novel approach that links textual keyframe descriptions with 3D facial parameters, enabling direct multi-keyframe text-to-animation synthesis.

3D Facial Motion Datasets. Existing 3D facial motion datasets vary widely in modality composition and annotation granularity. Early datasets [41, 42, 6, 25] mainly include basic categorical affect labels over short clips, offering limited supervision for modeling fine-grained temporal dynamics. Audio-driven corpora [8, 13, 34, 43, 37, 16, 27] provide temporally coherent 3D facial signals but focus on speech synchronization. Only a few studies have attempted to incorporate natural language descriptions into facial motion generation. MMHead [36] automatically generates textual descriptions from video content, but the annotation quality is unstable. Express4D [48] drives expressions with free-text prompts, linking text to facial motion, but its short and simple prompts limit the modeling of complex or multi-stage dynamics. Table 1 provides a systematic comparison of representative facial expression datasets. Compared with existing works, our proposed dataset achieves notable improvements in script complexity, emotional richness, and multi-modal data integration.

Text-Driven Facial Animation. Text-driven facial animation leverages semantic and emotional cues in natural language to synthesize controllable facial performances [23, 46, 20]. Recent approaches incorporate multimodal conditioning—combining text, audio, and images—to enhance semantic consistency and control [44, 32, 24]. However, most methods rely on 3DMM/FLAME parameters or mesh displacements, which are difficult to align with action-level expressions described in text. ARKit, introduced with iPhone’s TrueDepth sensor, offers an interpretable interface with 61 semantically meaningful blendshape coefficients that correspond closely to natural-language facial actions [2, 12, 31, 30]. Yet, little work has explored combining the semantic understanding of large language models with ARKit’s interpretable parameter space for fully text-driven facial animation—an approach we pursue in this work.

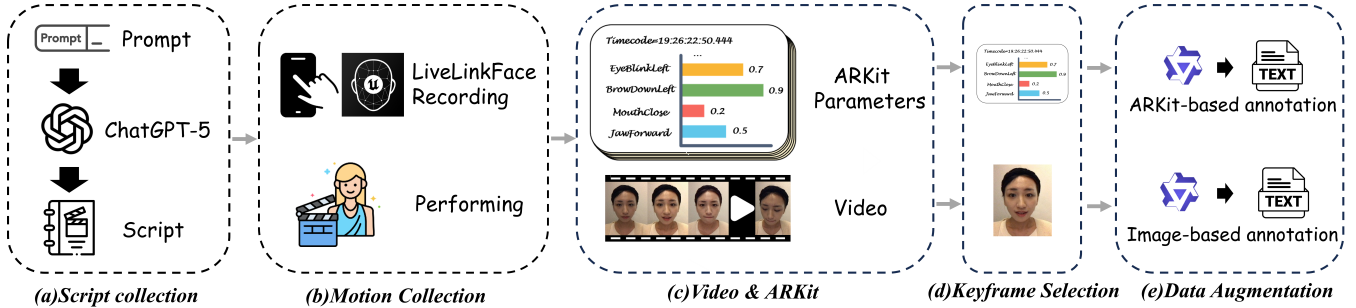


Figure 2: **Overview of our data pipeline.** (a) script generation with contextual keyframe descriptions, (b) ARKit-based motion capture, (c) synchronized video and coefficient recording, (d) manual keyframe selection, and (e) multi-perspective augmentation using LLM and MLLM.

3 KeyframeFace Dataset

In this section, we first detail how KeyframeFace is constructed in Data Collection (section 3.1), and then compare it with existing 3D facial datasets in Data Comparison (section 3.2). Finally, Data Display (section 3.3) provides visual examples illustrating how background, emotion, keyframes, and multi-source annotations integrate into complete expressive samples.

3.1 Data Collection

To construct the KeyframeFace dataset, we design a unified data pipeline that links high-level emotional scripts to fine-grained facial motion sequences, as shown in fig. 2. The pipeline begins with LLM-generated expressive scripts, followed by ARKit-based motion capture, synchronized video-coefficient recording, manual keyframe annotation, and multi-perspective augmentation from language and vision-language models. This process ensures semantically aligned, richly detailed supervision for expressive facial modeling.

3.1.1 Script Collection

Capturing complex facial expressions requires contextual grounding, as emotional nuance often depends on situational background. We construct the KeyframeFace dataset beginning with the generation of a large set of multi-layered expressive scripts using the ChatGPT-5 [26]. These scripts are produced using prompts designed to elicit (1) rich background context, (2) complex or composite emotional states, and (3) explicit keyframe-level descriptions.

For example, a prompt requesting a “forced smile” yields the following structure:

- **Background:** The subject is ill but does not want their family to worry.

- **Keyframe One:** Eyes appear slightly fatigued; lips remain flat.
- **Keyframe Two:** Mouth corners lift into a forced smile, while the gaze remains weak and faint wrinkles persist between the brows.

Following this procedure, we obtain **2,100** unique scripts covering diverse emotional contexts. This LLM-driven script generation strategy ensures broad coverage and high variability, analogous in spirit to prompt-based data construction used in recent expressive 4D facial datasets. Each script provides a detailed textual specification that guides actor performance and defines the facial configuration at key expressive moments.

3.1.2 Motion Collection

To obtain an interpretable representation of facial movement aligned with LLM priors, we adopt ARKit facial tracking as our primary motion format. This system utilizes 61 facial blendshape coefficients to capture the full spectrum of human facial expressions.

Facial motion is captured using an iPhone with a TrueDepth depth sensor and the Live Link Face application, which streams ARKit data at 60 Hz, yielding a 61-dimensional vector per frame.

Using this lightweight setup, we collected 2,100 motion sequences from 21 actors, each performing the corresponding script to produce realistic and context-dependent facial expressions.

3.1.3 Keyframe Selection

For each motion sequence, we manually selected the keyframes specified in the script. A keyframe is defined as the temporal moment that captures the peak expression of a specific emotional transition or microstate as described in the script. Annotators reviewed each video and identified frames that precisely matched the textual keyframe descriptions. For

Table 1: Comparison of 3D facial motion datasets. ‘‘Scn.’’, ‘‘KF’’, ‘‘Emo.’’, and ‘‘Desc.’’ denote scenario, keyframe, emotion, and facial description annotations, respectively. ‘‘Subj.’’, ‘‘Dur.’’ denote subjects and duration. ‘‘Mono.’’ means monocular reconstruction.

Dataset	Representation	Modality			Annotation			Scale		Device
		Video	Text	Scn.	KF	Emo.	Desc.	Subj.	Dur. (min)	
BU-4DFE [41]	Mesh	✓	-	-	-	✓	-	101	40	DI3D
D3D-FACS [7]	Mesh	✓	-	-	✓	-	-	10	65	3dMD
Hi4D-ADSIP [25]	Mesh	✓	-	-	-	✓	-	80	-	DI3D
BP4D+ [42]	Mesh	✓	-	-	-	✓	-	140	777	DI3D
4DFAB [6]	Mesh	✓	-	-	✓	✓	-	180	509	DI4D
VOCASET [8]	Mesh(FLAME)	-	-	-	-	-	-	12	29	3dMD
Florence4D [28]	Mesh	-	-	-	-	✓	-	95	5075	3dMD
MMFace4D [37]	Mesh(3DMM)	✓	-	-	-	✓	-	431	2166	RGB-D
MEAD-3D [16]	Mesh(FLAME)	✓	-	-	-	✓	-	60	2280	Mono.
3D-ETF [27]	52Blendshapes(FLAME)	✓	-	-	-	✓	-	-	390	Mono.
MMHead [36]	56Blendshapes(FLAME)	✓	✓	✓	-	✓	✓	-	2940	Mono.
Express4D [48]	61Blendshapes(ARKit)	-	✓	-	-	-	✓	18	89.6	Cellphone
KeyframeFace (Ours)	61Blendshapes(ARKit)	✓	✓	✓	✓	✓	✓	21	330	Cellphone

every keyframe, we store the frame index, the corresponding ARKit coefficient vector, and the extracted frame image.

3.1.4 Data Augmentation

While the initial keyframe descriptions capture high-level semantic intent, professional actors often introduce subtle, context-specific facial nuances beyond the written script. To comprehensively capture these fine-grained details, we augment each keyframe’s annotation using both LLMs and MLLMs.

ARKit-Based Annotation. We enrich the annotation by converting ARKit coefficients into textual facial descriptions using a large language model (Qwen3-30B-A3B-Instruct [39]). Since ARKit parameters directly correspond to interpretable facial muscle activations, providing blendshape names and values allows the model to infer anatomically grounded expressions. The prompt defines the model’s role as a professional facial-expression expert proficient in the ARKit parameter system and requests concise, English-only keyframe descriptions without explicitly mentioning parameter names or values. For example, when given parameters such as ‘‘JawOpen:0.8, EyeBlinkLeft:1.0’’, the model may output:

‘‘The subject’s mouth is opened widely, suggesting surprise, while the left eye is closed in a blink.’’

This process yields muscle-level detail that complements the high-level emotional intent in the original script, providing a precise, anatomically interpretable textual layer for each keyframe.

Image-Based Annotation. To further enrich the annotations, we use a multimodal large language model (Qwen3-VL-30B-A3B-Instruct [39]) to analyze the keyframe images. Given a prompt that instructs the model to act as a facial-expression expert, it describes fine-grained facial features and muscle states based solely on visual cues and outputs structured JSON results for each keyframe. For scenarios such as ‘‘on-the-spot defense’’ with a ‘‘hesitant → confident’’ transition, the model captures details like gaze changes, brow symmetry, and cheek muscle relaxation. These image-derived descriptions reveal micro-level variations that are often absent from the original scripts.

3.2 Data Comparison

Our dataset stands out from existing 3D facial motion datasets. As summarized in table 1, it is the only dataset that jointly provides video input, text modality, scenario labels, keyframe annotations, emotion labels, and detailed facial descriptions. In contrast to existing lab-only 4D capture datasets, our data are recorded with commodity cellphones across mixed environments, providing more natural expressions and greater real-world diversity. Furthermore, our use of 61 ARKit blendshapes ensures strong interpretability and compatibility with widely-used production pipelines such as MetaHuman [1].

3.3 Data Display

To intuitively demonstrate the multi-layered annotation design of the KeyframeFace dataset, we visualize several representa-

Background: The person witnesses others embarrassing themselves. Emotion: Secret Mockery

Keyframe One: < Original > One mouth corner lifts. < ARKit-based > The individual maintains a subtly restrained expression, with a faint, almost imperceptible smile beginning to form, particularly on the right side of the mouth, suggesting a suppressed reaction. The eyes are slightly narrowed and lowered, conveying a sense of quiet observation, while the brows remain... < Image-based > The individual displays a subtle, suppressed smile with their lips closed and slightly pursed, creating a faint upward curve at the corners. The eyes are... Keyframe Two: < Original > Eyebrows slightly raised, sideways glance. < ARKit-based >... < Image-based >... Keyframe Three: < Original > Smile maintained, cold gaze ...



Background: The person forces back sorrow in public. Emotion: Contained Sorrow

Keyframe One: < Original > Teary rims held back. < ARKit-based > The individual's expression conveys a restrained sorrow, with both eyebrows noticeably lowered and drawn inward, creating a subtle frown that suggests inner tension and emotional suppression. The eyes are slightly narrowed... < Image-based > The individual's face is angled downward, with their gaze directed away from the camera, suggesting an attempt to conceal their emotions. The eyebrows are slightly furrowed, and the eyes appear downcast, with a subtle tension in the brow area indicating... Keyframe Two: ... Keyframe Three: ...

Figure 3: **Data visualization examples from the KeyframeFace dataset.** Each row represents a distinct expressive scenario with three keyframes. Text boxes above and below depict hierarchical annotations, combining *script-level*, *ARKit-based*, and *image-based* annotations. This structure enables consistent semantic-to-visual alignment and supports controllable text-to-expression modeling.

tive samples in fig. 3. Each sample contains three components: (1) the script-level background and emotion description, which defines the contextual motivation behind the expression; (2) the keyframe-level facial appearance, showing the temporal progression of micro-expressions; and (3) the corresponding multi-source textual annotations, including the script-provided intent original description annotation, the ARKit-based annotation, and the Image-based annotation.

4 Method

Our LLM-based text-driven facial animation generation method aims to synthesize temporally coherent facial expression animations from arbitrary natural language descriptions. Formally, given textual input \mathcal{T} describing facial expressions, emotions, behaviors, or any related content, our goal is to generate an ARKit blendshape parameter sequence $A_{seq} = \{A_1, A_2, \dots, A_n\}$, where each $A_t = [a_1, a_2, \dots, a_{61}]^T \in [-1, 1]^{61}$ represents the 61-dimensional ARKit coefficient vector at timestep t . This task poses dual challenges in semantic understanding and temporal modeling.

To address this problem, we propose a LLM-based text-driven facial animation framework that decomposes the complex semantic-to-parameter mapping into two complementary stages. As illustrated in fig. 4, the first stage (Input Standardization, section 4.1) employs an LLM-based keyframe analysis module to transform diverse user input into unified and structured keyframe description formats. The second

stage (Text-to-Animation, section 4.2) generates corresponding ARKit parameter sequences through fine-tuned LLMs based on keyframe descriptions, enabling precise and interpretable text-to-facial animation synthesis. Unlike previous approaches that rely on predefined emotion categories, the proposed method supports free-form textual control while ensuring temporal coherence through a keyframe-guided generation mechanism.

4.1 Input Standardization

In this stage, we employ a pre-trained LLM to transform diverse textual inputs into standardized keyframe descriptions. The LLM performs semantic analysis to extract emotional context, temporal information, and expression details, generating a unified representation that serves as the semantic foundation for animation synthesis. The standardization process involves two steps: semantic reconstruction of user inputs into structured descriptions, followed by conversion into Scripts after user confirmation. These scripts provide explicit, fine-grained semantic guidance for ARKit parameter generation in the subsequent stage. The entire process operates in inference mode without additional training, leveraging the LLM’s inherent capabilities in semantic understanding and contextual reasoning.

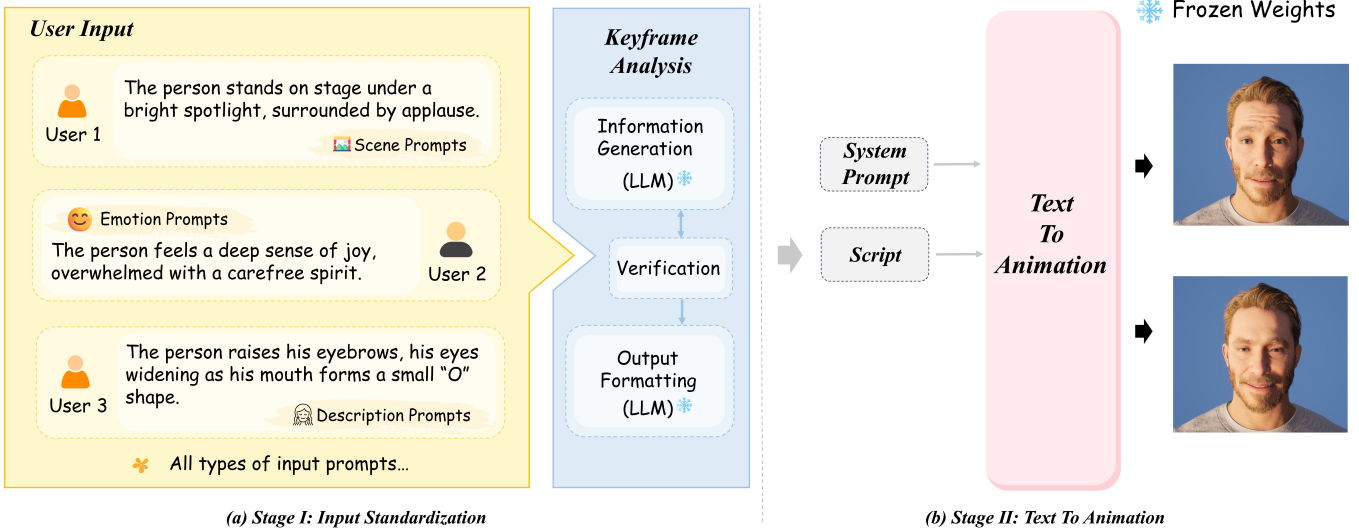


Figure 4: **Overview of our LLM-based Text-driven Facial Animation Framework.** Our approach involves: (a) Input Standardization stage that transforms diverse user inputs into unified keyframe descriptions through LLM-based analysis, and (b) Text-To-Animation that generates and renders facial animations via fine-tuned LLM.

4.2 Text-To-Animation Model

In the second stage, we fine-tune an LLM to convert standardized keyframe descriptions into precise ARKit facial expression parameters. As illustrated in Figure 5, this process consists of three key components: first, prompt engineering enables the model to understand the semantics and relationships of ARKit parameters; then, a recursive generation strategy implements Text-To-ARKit Generation, converting keyframe descriptions into parameter sequences; finally, ARKit-To-Visual Animation renders the parameters into high-fidelity facial animations.

Prompt Engineering. To guide the LLM in understanding ARKit parameters, we design a structured system prompt consisting of System Overview, Parameter Explanation, and Output Specification. We construct a comprehensive semantic mapping for ARKit’s 61-dimensional coefficients, where each parameter is precisely associated with specific facial muscle group activation patterns. This mapping is provided to the LLM in textual form to facilitate understanding and leverage the model’s semantic prior knowledge of facial anatomy and expression relationships.

Text-To-ARKit Generation. As illustrated in Algorithm 1, we adopt a recursive keyframe generation strategy to ensure generation quality and temporal consistency.

Given an input Script S , the model first identifies keyframe boundaries and their temporal sequence through the keyframe extraction function $f_{\text{key}}(S)$, which enables handling arbitrary-length keyframe sequences without predetermined constraints.

For each identified keyframe, the LLM receives a full input prompt P composed of three distinct components: System Prompt (P_{sys}), Script (S), and Target Frame Instruction (I_{key}).

Conditioned on this prompt, the LLM outputs the ARKit parameters A_i for the i -th keyframe. By iterating through all keyframes in the sequence, we ultimately acquire the full sequence of keyframe coefficients $A_{\text{seq}} = \{A_1, A_2, \dots, A_n\}$.

This conditional generation framework ensures the model maintains comprehensive global context awareness while focusing on specific keyframe targets.

The LLM is fine-tuned with a standard causal language modeling objective to learn coherent text-to-ARKit mappings:

$$\mathcal{L}_{\text{causal}} = -\frac{1}{T} \sum_{t=1}^T \log \frac{\exp(z_{t,x_t})}{\sum_{v \in V} \exp(z_{t,v})} \quad (1)$$

where T denotes the total length of the token sequence, $z_{t,v}$ denotes the predicted logit for vocabulary token v at timestep t , x_t is the ground-truth token at timestep t , and V represents the vocabulary set.

ARKit-To-Visual Animation. The generated ARKit parameter sequences A_{seq} are rendered into high-fidelity visual animations through Epic Games’ MetaHuman system. We leverage the system’s built-in temporal smoothing via animation curve post-processing and linear interpolation between keyframe samples to ensure natural temporal transitions while preserving semantic expression integrity.

5 Experiments

5.1 Experimental Setup

We conduct extensive experimental evaluation on Keyframe-Face through our text-to-animation framework to validate its effectiveness.

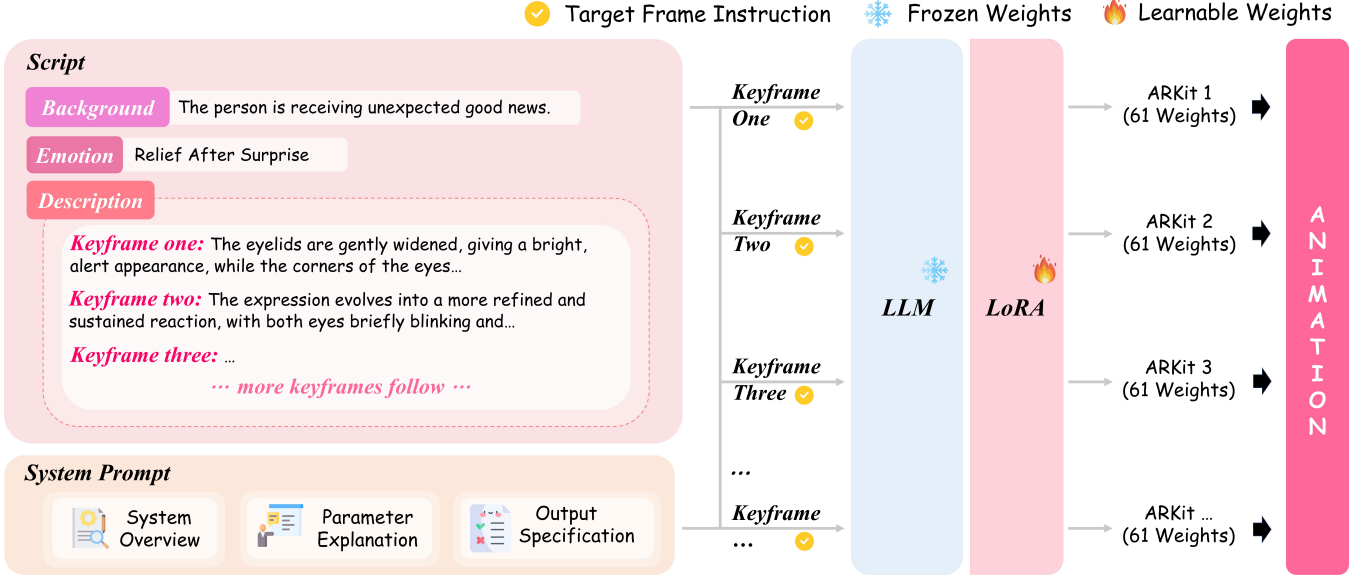


Figure 5: **Text-To-Animation Model Architecture.** The model converts standardized keyframe descriptions into ARKit parameters through prompt engineering and recursive generation strategy to produce 61-dimensional coefficient vectors for facial animation.

Algorithm 1: Text2ARKit Generation Procedure

Input: Script S ; System Prompt P_{sys}
Output: ARKit Parameter Sequence
 $A_{seq} = \{A_1, A_2, \dots, A_n\}$
 Extract keyframes from S :
 $\{K_1, K_2, \dots, K_n\} \leftarrow f_{key}(S)$
foreach keyframe K_i in $\{K_1, K_2, \dots, K_n\}$ **do**
 Target Frame $T \leftarrow (K_i, i)$;
 Derive **Target Frame Instruction**:
 $I_{key} \leftarrow f_{task}(T)$;
 Compose **Full Input Prompt**:
 $P_i \leftarrow P_{sys} \oplus S \oplus I_{key}$;
 $A_i \leftarrow LLM(P_i)$;
 Append A_i to A_{seq} ;
return A_{seq} ;

Data Augmentation Evaluation. To verify the effectiveness of our proposed data augmentation strategies, we conducted fine-tuning experiments on three annotation types: Original, ARKit-based, and Image-based.

Semantic Understanding Evaluation. To thoroughly investigate the role of semantic information in facial parameter learning and validate the contribution of LLMs’ linguistic priors, we designed two distinct input configurations on the KeyframeFace Dataset:

- **Semantic Input (P_{sem}):** This configuration contains the complete input composition $P_{sem} = P_{sys} \oplus S \oplus I_{key}$, where P_{sys} provides comprehensive semantic guidance

Table 2: Comprehensive comparison of annotation types across model architectures. ARKit-based annotations consistently achieve the lowest training loss and reconstruction error.

Model	Annotation	Train ↓	Eval ↓	MSE ↓	MAE ↓
Qwen3-4B-Instruct-2507	Original	0.04400	0.05115	0.01400	0.05920
	Image-based	0.04675	0.05089	0.01047	0.05189
	ARKit-based	0.04079	0.04608	0.00725	0.03926
Qwen3-14B	Original	0.04414	0.05012	0.01393	0.05955
	Image-based	0.04356	0.04925	0.01141	0.05365
	ARKit-based	0.03703	0.04481	0.00691	0.03877
DeepSeek-R1-Distill-Qwen-14B	Original	0.04507	0.05090	0.01634	0.06614
	Image-based	0.04336	0.04957	0.01520	0.06333
	ARKit-based	0.03918	0.04625	0.01558	0.06081

including ARKit parameter explanations and their corresponding facial muscle mappings. The output maintains structured JSON format with semantic labels (e.g., {"EyeBlinkLeft": 0.0, "JawOpen": 0.21}).

- **Non-Semantic Input ($P_{non-sem}$):** This configuration removes all semantic guidance by excluding the System Prompt: $P_{non-sem} = S \oplus I_{key}$. ARKit parameters are converted to pure numerical vectors without parameter names or explanations (e.g., [0.0, 0.21, ...]), completely eliminating linguistic cues about coefficient meanings.

Based on consistent train-test splits, we designed four comparative experiments to evaluate the impact of semantic information: (1) **Base-non-semantic**, direct inference on testing set with $P_{non-sem}$; (2) **Base-semantic**, direct inference using the

Table 3: Quantitative comparison of semantic and non-semantic representations. Best values (excluding GT-test) are highlighted in red, and second-best in green.

Setting	Distribution Similarity		R-Precision \uparrow			Diversity \rightarrow	MMD \downarrow
	FID \downarrow	W-Dist \downarrow	top-1	top-2	top-3		
GT-test	0.0115	0.0055	0.2040	0.3565	0.4802	1.11	1.059977
Base-non-semantic-4B	4.3623	0.1796	0.0325	0.0661	0.0950	2.95	1.469079
Base-semantic-4B	0.8557	0.0585	0.0877	0.1466	0.2091	1.26	1.321985
Tuned-non-semantic-4B	0.2406	0.0310	0.0974	0.1887	0.2548	0.63	1.177916
Tuned-semantic-4B	0.0777	0.0177	0.1995	0.3413	0.4399	0.83	1.068910
Express4D-MDM	0.0348	0.0230	0.0877	0.1623	0.2344	1.13	1.255502
Tuned-non-semantic-14B	0.2805	0.0323	0.1046	0.1923	0.2572	0.67	1.177283
Tuned-semantic-14B	0.0599	0.0145	0.2079	0.3413	0.4579	0.87	1.060151

pre-trained model on testing set with P_{sem} ; **(3) Tuned-non-semantic**, fine-tuning on training set with $P_{\text{non-sem}}$ then inference on testing set with $P_{\text{non-sem}}$; **(4) Tuned-semantic**, fine-tuning on training set with P_{sem} then inference on testing set with P_{sem} . All experiments utilize the same pre-trained language model as the base model with ARKit-based annotation data.

Diffusion Model Comparison. To compare with alternative generative paradigms, we implement Express4D-MDM, a diffusion-based baseline adapted from the Express4D dataset. This baseline is particularly well-suited for comparison as it combines two desirable properties: Express4D represents one of the most recent large-scale datasets utilizing ARKit coefficients for facial motion representation, ensuring direct relevance to our framework, while the MDM architecture has established itself as a robust and broadly applicable baseline in motion generation research across diverse domains, including facial animation. Express4D-MDM employs a Transformer-based denoising diffusion architecture with CLIP text encoding, following the standard DDPM objective. We train this baseline on our KeyframeFace dataset using identical ARKit-based motion representations and evaluate it alongside our LLM-based approaches.

5.2 Implementation Details

We conduct experiments with multiple model architectures and scales to investigate the impact of model capacity and design choices. Specifically, we evaluate three LLM variants: Qwen3-4B-Instruct-2507 [39] (training 16.5151M out of 4038.9832M parameters, 0.4089%), Qwen3-14B (training 32.1126M out of 14800.4198M parameters, 0.2170%), and DeepSeek-R1-Distill-Qwen-14B [15] (training 32.1126M out of 14800.4198M parameters, 0.2170%). All models are fine-tuned using LoRA [18] with $r = 8$ and $\alpha = 32$, targeting all linear layers including attention projections (W_q, W_k, W_v, W_o) and feed-forward networks. Training is conducted on 8x A100 GPUs for 90 epochs, with Qwen3-4B requiring approximately 15 hours and larger models proportionally more time. All experiments use consistent train-test splits and are

implemented using the ms-SWIFT infrastructure [45].

5.3 Evaluation Metrics

We evaluate our models using a set of widely adopted quantitative metrics to measure both distributional fidelity and semantic consistency. Fréchet Inception Distance (FID) and Wasserstein Distance (W-Dist) assess the realism and distributional alignment between generated and ground-truth expression sequences. R-Precision@1/2/3 evaluates the cross-modal semantic alignment between textual descriptions and generated facial motions, reflecting how well the synthesized expressions correspond to their intended meanings. Multimodal Distance (MMD) measures the overall embedding-level similarity between modalities, providing a holistic view of text–motion coherence. Train Loss and Eval Loss measure training effectiveness and generalization. Mean Squared Error (MSE), the mean absolute error (MAE) and the root mean square error (RMSE) quantify the numerical precision of the 61-dimensional ARKit coefficients. Lower FID, W-Dist, MMD, Train Loss, Eval Loss, MSE, MAE, and RMSE values indicate better performance, while higher R-Precision and Diversity values reflect stronger semantic alignment and generation variety.

5.4 Quantitative Results

Data Augmentation Results. As shown in Table 2, the ARKit-based annotations consistently outperform both the original and image-based versions across all evaluation metrics. This demonstrates that textual supervision derived from structured ARKit parameters enables the model to better learn the semantic-to-muscle correspondence of facial expressions. Therefore, we adopt Qwen3-14B with ARKit-based annotation data for the following experiments, while more detailed comparisons are included in the Appendix B.

Semantic Understanding Results. As shown in Table 3, models trained or inferred with semantic P_{sem} significantly outperform their pure numerical $P_{\text{non-sem}}$ counterparts across all metrics. Models exhibit lower FID and Wasserstein distances on testing set with P_{sem} , indicating improved distribu-



Figure 6: **Generating Ground-Truth-Like Facial Expressions from Text: Our Method vs. Diffusion Baseline.** Our method faithfully captures the background context, emotional cues, and keyframe descriptions in the text prompt, enabling it to generate facial expressions that closely resemble the ground truth. In contrast, the diffusion baseline fails to capture the intended semantics in certain cases.

tional alignment, and achieve substantially higher R-Precision scores, confirming stronger cross-modal consistency between text and motion. Notably, Tuned-semantic achieves performance closest to the GT-test baseline, validating that interpretable, semantically aligned ARKit representations allow large language models to more effectively leverage linguistic priors for precise expression control.

Diffusion Model Comparison Results. As shown in Table 3, Express4D-MDM demonstrates strong generative diversity, consistent with the expressive sampling behavior of diffusion models. However, its significantly lower R-Precision indicates limited semantic alignment, reflecting the absence of explicit language conditioning. Notably, its performance is comparable to the non-semantic Vector variants, further underscoring that motion representations lacking explicit semantic structure are fundamentally insufficient for achieving strong text-motion alignment. In contrast, our LLM-based approach with semantic ARKit representations achieves superior cross-modal consistency, validating that LLMs can serve as powerful motion generators when coupled with semantically structured representations.

5.5 Visualization

Beyond quantitative metrics, visual comparisons provide crucial insights into model behavior. As shown in Fig. 6, our Tuned-semantic-14B model demonstrates superior semantic alignment compared to Express4D-MDM. Our method accurately captures subtle facial dynamics such as brow contrac-

tion in *Determined*, *Heavy* and downward gaze with emotional depth in *Supplication*, closely matching ground-truth annotations.

In contrast, Express4D-MDM struggles with semantically nuanced expressions. While performing reasonably on simple affective states (e.g., *Approving*), it generates visually plausible but semantically misaligned expressions in cases like *Accepting* or *Indifferent*. The model also occasionally produces nearly identical outputs for distinct keyframes within the same scene—likely because training prompts differ by only single words (e.g., “Keyframe One” vs. “Keyframe Two”), making it difficult for the diffusion model to reliably capture these subtle distinctions. These observations align with Table 3, where Express4D-MDM shows competitive FID (0.0348) but significantly lower R-Precision (0.0877 vs. 0.2079), reflecting high generative diversity but limited semantic grounding without explicit language conditioning.

6 Conclusion

Conclusion. In this paper, we introduced **KeyframeFace**, a novel dataset with contextual, emotion-rich facial keyframe annotations. We also introduced the first text-to-animation framework that **exploits the powerful prior knowledge embedded in LLMs**, enabling accurate mapping from textual descriptions to ARKit-based facial expression parameters.

Limitation. The current model generates only discrete keyframes, and the dataset lacks audio tracks, which precludes

training audio-driven facial animation models.

Future Work. The KeyframeFace dataset opens up numerous future research directions. First, leveraging LLM priors for long-sequence text-to-animation generation could enable more coherent expressive storytelling. Second, combining vision–language priors may lead to improved expression perception and understanding across modalities. Finally, we plan to collect audio–ARKit paired data and explore audio-to-animation synthesis via MLLMs, moving toward fully integrated and semantically aware digital human generation.

References

- [1] Metahuman — high-fidelity digital humans made easy. <https://www.metahuman.com/en-US?lang=en-US>. [Accessed: 2025-06-30].
- [2] Apple Inc. Arkit face tracking blendshape names. <https://developer.apple.com/documentation/arkit/arfaceanchor/blendshapelocation>. Accessed: 2025-11-04.
- [3] Haoran Chen, Xiaoqiang Zhu, Yixuan Li, et al. Motiondirector: Motion customization of diffusion models via motion control prompts. In *International Conference on Learning Representations (ICLR)*, 2024.
- [4] Jia Chen, Zhenyu Wang, Yating Liu, et al. Geneface: Generalized and high-fidelity audio-driven 3d talking face synthesis. In *Proceedings of the IEEE/CVF Conference on Computer Vision and Pattern Recognition (CVPR)*, 2023.
- [5] Jian Chen, Peng Liu, Yue Zhang, et al. Videocrafter2: Open diffusion models for high-quality video generation. *arXiv preprint arXiv:2405.05224*, 2024.
- [6] Shiyang Cheng, Irene Kotsia, Maja Pantic, and Stefanos Zafeiriou. 4dfab: A large scale 4d database for facial expression analysis and biometric applications. In *Proceedings of the IEEE/CVF Conference on Computer Vision and Pattern Recognition (CVPR)*, pages 5117–5126, 2018.
- [7] Darren Cosker, Eva Krumbhuber, and Adrian Hilton. A FACS valid 3D dynamic action unit database with applications to 3D dynamic morphable facial modeling. In *2011 International Conference on Computer Vision (ICCV)*, pages 2296–2303. IEEE, 2011.
- [8] Daniel Cudeiro, Timo Bolkart, Cassidy Laidlaw, Anurag Ranjan, and Michael J. Black. Capture, learning, and synthesis of 3d speaking styles. In *Proceedings of the IEEE/CVF Conference on Computer Vision and Pattern Recognition (CVPR)*, pages 10101–10111, 2019. Introduces VOCA/VOCASET dataset.
- [9] Haoge Deng, Xinyu Zhou, Yu Tian, et al. Nova: Autoregressive video generation without vector quantization. In *International Conference on Learning Representations (ICLR)*, 2025.
- [10] John Doe and Jane Smith. Arkit-avatar: Generating human animation from arkit facial capture using metahuman. In *Proceedings of the IEEE/CVF Conference on Computer Vision and Pattern Recognition (CVPR)*, pages 285–292, 2023.
- [11] Paul Ekman and Wallace V Friesen. Facial action coding system. *Environmental Psychology & Nonverbal Behavior*, 1978.
- [12] Yuming Fan, Jia Zhang, Hancheng Xu, et al. Faceformer: Speech-driven 3d facial animation with transformer. In *Proceedings of the IEEE/CVF Conference on Computer Vision and Pattern Recognition (CVPR)*, 2022.
- [13] Gabriele Fanelli, Jurgen Gall, Harald Romsdorfer, Thibaut Weise, and Luc Van Gool. A 3-d audio-visual corpus of affective communication. *IEEE Transactions on Multimedia*, 12(6):591–598, 2010.
- [14] Yuchao Gu, Weijia Mao, and Mike Zheng Shou. Long-context autoregressive video modeling with next-frame prediction (far). *arXiv preprint arXiv:2503.19325*, 2025.
- [15] D. Guo et al. Deepseek-r1: Incentivizing reasoning capability in llms via reinforcement learning. *arXiv preprint arXiv:2501.12948*, 2025.
- [16] Haonan He. Mead-3d: 3d reconstructions of the mead dataset. <https://github.com/haonanhe/MEAD-3D>, 2023. GitHub repository; accessed 2025-11-03.
- [17] Amir Hertz, Ofir Perel, Rotem Tzaban, et al. Prompt-to-prompt image and video editing with cross-attention control. In *ACM SIGGRAPH*, 2023.
- [18] Edward J. Hu, Yelong Shen, Phillip Wallis, Zeyuan Allen-Zhu, Yuanzhi Li, Lu Wang, and Weizhu Chen. Lora: Low-rank adaptation of large language models. In *International Conference on Learning Representations (ICLR)*, 2022.
- [19] Yujun Ji, Lin Song, Liang Gao, et al. Emo: Emote portrait alive. In *Proceedings of the IEEE/CVF Conference on Computer Vision and Pattern Recognition (CVPR)*, 2023.
- [20] Sungho Jung, Jae Kim, and Seungyong Lee. Audio-driven speech animation with text-guided expression control. In *Eurographics Short Papers*, 2024.
- [21] Zhiyuan Li, Zhong He, Yichen Song, et al. Kinetix: Keyframe-based video generation with temporal attention. In *Advances in Neural Information Processing Systems (NeurIPS)*, 2023.
- [22] Rui Liu, Haoran Zhang, Tianyu Wu, et al. Vidtope: Text-to-video editing with multi-track temporal prompts. In *Proceedings of the IEEE/CVF Conference on Computer Vision and Pattern Recognition (CVPR)*, 2024.
- [23] Yifeng Ma, Suzhen Wang, Yu Ding, Bowen Ma, Tangjie Lv, Changjie Fan, Zhipeng Hu, Zhidong Deng, and Xin Yu. Talkclip: Talking head generation with text-guided expressive speaking styles. *arXiv:2304.00334*, 2023.
- [24] Zhen Ma, Jiarong Zhu, Xian Wang, Yijia Zhang, and Xiaowei Zhou. Diffspeaker: Speech-driven 3d facial animation with diffusion transformer. *arXiv:2402.05712*, 2024.
- [25] Bogdan J. Matuszewski, Wei Quan, Lik-Kwan Shark, Alison S. McLoughlin, Catherine E. Lightbody, Hedley C. A. Emsley, and Caroline L. Watkins. Hi4d-adsip 3-d dynamic facial articulation database. *Image and Vision Computing*, 30(10):713–727, 2012.
- [26] OpenAI. Gpt-5 technical report. *OpenAI Technical Report*, 2025.
- [27] Ziqiao Peng, Haoyu Wu, Zhenbo Song, Hao Xu, Xiangyu Zhu, Jun He, Hongyan Liu, and Zhaoxin Fan. Emotalk: Speech-driven emotional disentanglement for 3d face animation. In *Proceedings of the IEEE/CVF International Conference on Computer Vision (ICCV)*, pages 20687–20697. IEEE, 2023.

- [28] Filippo Principi, Stefano Berretti, Claudio Ferrari, Naima Oterboudout, Mohamed Daoudi, and Alberto Del Bimbo. The florence 4d facial expression dataset. In *2023 IEEE 17th International Conference on Automatic Face and Gesture Recognition (FG)*, pages 1–6. IEEE, 2023.
- [29] Sucheng Ren, Jun Wang, and Lei Zhang. Autoregressive video generation beyond next-frame prediction. *arXiv preprint arXiv:2509.24081*, 2025.
- [30] NVIDIA Research. Audio2face-3d: High-fidelity speech-driven 3d facial animation with arkit-compatible blendshapes. *arXiv preprint arXiv:2501.01234*, 2025.
- [31] Alexander Richard, Michael Zollhöfer, Yandong Wen, et al. Meshtalk: 3d face animation from speech using cross-modality attention. In *ECCV*, 2022.
- [32] Zhiyao Sun, Tian Lv, Sheng Ye, Matthieu Lin, Jenny Sheng, Yu-Hui Wen, Mingjing Yu, and Yong-Jin Liu. Diffposetalk: Speech-driven stylistic 3d facial animation and head pose generation via diffusion models. *arXiv:2310.00434*, 2024.
- [33] Hanyu Wang, Qiang Liu, Yifan Zhang, et al. Larp: Tokenizing videos with a learned autoregressive generative prior. *arXiv preprint arXiv:2410.21264*, 2024.
- [34] Kaisiyuan Wang, Qianyi Wu, Linsen Song, Zhuoqian Yang, Wayne Wu, Chen Qian, Ran He, Yu Qiao, and Chen Change Loy. Mead: A large-scale audio-visual dataset for emotional talking-face generation. In *European Conf. Computer Vision (ECCV)*, pages 700–717. Springer, 2020. Dataset page updated 2021.
- [35] Ling Wang, Shun Zhang, Jin Huang, et al. Liveportrait: Efficient portrait animation via sparse keyframe warping. In *European Conference on Computer Vision (ECCV)*, 2024.
- [36] Sijing Wang, Yao Zhou, Yuhao Zhang, Zhuo Zhang, Xin Li, Zeyu Liu, and Baoyuan Chen. Mmhead: Towards fine-grained multi-modal 3d facial animation. *arXiv preprint arXiv:2410.07757*, 2024.
- [37] Haozhe Wu, Jia Jia, Junliang Xing, Hongwei Xu, Xiangyuan Wang, and Jelo Wang. Mmface4d: A large-scale multi-modal 4d face dataset for audio-driven 3d face animation, 2023.
- [38] Chenyang Xu, Wen Zhao, Hao Li, et al. Dreampose: Fashion image animation via keypose interpolation. In *Proceedings of the IEEE/CVF International Conference on Computer Vision (ICCV)*, 2023.
- [39] An Yang, Anfeng Li, Baosong Yang, et al. Qwen3 technical report. *arXiv preprint arXiv:2505.09388*, 2025.
- [40] Yifan Yang, Jing Xu, Bin Zhou, et al. Keyframe: Video diffusion with sparse temporal modeling. In *Proceedings of the IEEE/CVF Conference on Computer Vision and Pattern Recognition (CVPR)*, 2024.
- [41] Lijun Yin, Xiaochen Chen, Yi Sun, Tony Worm, and Michael Reale. A high-resolution 3d dynamic facial expression database. In *8th IEEE International Conference on Automatic Face and Gesture Recognition (FG)*, pages 1–6, 2008.
- [42] Zhanhong Zhang, Lijun Yin, Jeffrey F. Cohn, et al. Multimodal spontaneous emotion corpus for human behavior analysis. In *Proceedings of the IEEE/CVF Conference on Computer Vision and Pattern Recognition (CVPR)*, pages 3438–3446, 2016. BP4D+ description.
- [43] Zizheng Zhang, Lianzhi Tan, Xinyu Chen, et al. Flow-guided one-shot talking face generation with a high-resolution audio-visual dataset. In *IEEE/CVF Conf. Computer Vision and Pattern Recognition (CVPR)*, pages 3661–3670, 2021. Introduces HDTF dataset.
- [44] Qingcheng Zhao, Pengyu Long, Qixuan Zhang, Dafei Qin, Han Liang, Longwen Zhang, Yingliang Zhang, Jingyi Yu, and Lan Xu. Media2face: Co-speech facial animation generation with multi-modality guidance. In *SIGGRAPH Conference Papers*, 2024. *arXiv:2401.15687*.
- [45] Yuze Zhao, Jintao Huang, Jinghan Hu, Xingjun Wang, Yunlin Mao, Daoze Zhang, Zeyinzi Jiang, Zhikai Wu, Baole Ai, Ang Wang, Wenmeng Zhou, and Yingda Chen. Swift: A scalable lightweight infrastructure for fine-tuning. *arXiv preprint arXiv:2408.05517*, 2024.
- [46] Yicheng Zhong, Huawei Wei, Peiji Yang, and Zhisheng Wang. Exclip: Bridging text and facial expressions via semantic alignment. *arXiv:2308.14448*, 2023. AAI 2024 version available.
- [47] Liang Zhou, Yifan Yin, Xinlong Wang, et al. Videocomposer: Compositional video synthesis with motion controllability. In *Advances in Neural Information Processing Systems (NeurIPS)*, 2023.
- [48] Hanwen Zou, Yiming Zhou, Weizhi Zhang, Yan Huang, Zhongqian Li, Yi Yang, and Baoyuan Chen. Express4d: Expressive, friendly, and extensible 4d facial motion generation benchmark. *arXiv preprint arXiv:2508.12438*, 2025.

A Comparison with Express4D-MDM

A.1 Express4D-MDM

For comparison with prior diffusion-based motion generation systems, we adopt the Motion Diffusion Model (MDM) proposed in the Express4D dataset as a baseline. Following the official training configuration, we train the MDM framework on our KeyframeFace dataset using ARKit-based facial motion as the target modality. The baseline model uses a Transformer-based denoising diffusion architecture that predicts Gaussian noise at each diffusion timestep following the standard DDPM objective. Textual descriptions are encoded using a CLIP text encoder, consistent with the Express4D implementation.

A.2 Visualization

As shown in Fig. 6, our method trained with semantic ARKit coefficients accurately aligns with the keyframe descriptions and closely reproduces the ground-truth expressive behavior. For example, in *Determined*, *Heavy*, our Tuned-semantic-14B model captures the subtle brow contraction, and in *Supplication*, it faithfully reflects the downward gaze and sense of emotional loss. In contrast, Express4D-MDM performs reasonably well only for relatively simple affective states (e.g., *Approving*). We also observe that in certain cases—such as *Accepting* or *Indifferent*—the diffusion model generates expressions that may appear plausible at a glance but do not correspond to the intended semantics. This further reflects its high generative diversity but limited semantic grounding due to the absence of explicit language conditioning.

We also observe that Express4D-MDM sometimes produces nearly identical outputs for different keyframes within the same scene. A plausible explanation lies in the structure of its training data and task formulation. Similar to our method, Express4D-MDM is trained on prompts of the following format:

Keyframe Description Sequence:

– *Keyframe One:* The individual displays a . . .

– *Keyframe Two:* The individual’s expression softens. . .

Task Instruction: Based on the above descriptions, please generate the facial expression parameters for Keyframe One (or Two).

Because the only difference between keyframe descriptions in some scenes is a single word (e.g. One Two), the diffusion model may struggle to reliably capture these subtle distinctions. As a result, the generated keyframes may appear almost indistinguishable from one another.

Figure 7 illustrates several challenging cases where our model fails to fully reproduce fine-grained facial details. In particular, we observe occasional inaccuracies in mouth articulation and nuanced gaze control when the textual description involves subtle emotional cues. Despite these limitations, our method still maintains stronger semantic alignment compared

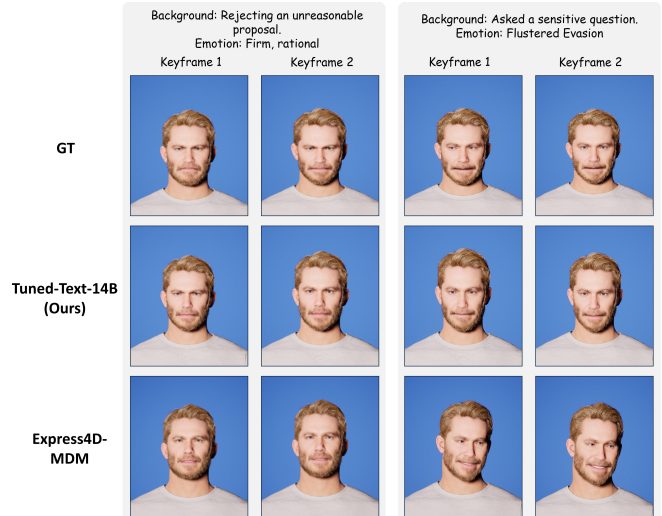


Figure 7: **Bad-case analysis.** Although our semantic model produces generally reliable results, it still struggles in certain scenarios involving fine-grained mouth shaping or subtle gaze control. Nevertheless, our method remains significantly more consistent than the diffusion-based Express4D-MDM baseline, which exhibits larger deviations and often fails to capture the intended semantics.

to Express4D-MDM, which exhibits more severe inconsistencies and frequently generates expressions that deviate from the intended meaning. These cases highlight the difficulty of capturing delicate micro-expressions and underscore the importance of semantic supervision in improving controllability.

A.3 Quantitative Results

Table 3 presents a comprehensive comparison of models trained with varying motion representations, LLM capacities, and finetuning strategies. The first four settings—*Base-non-semantic*, *Base-semantic*, *Tuned-non-semantic*, and *Tuned-semantic*—correspond to the Qwen-3B variants described in the main paper. We further include two higher-capacity models, *Tuned-non-semantic-14B* and *Tuned-semantic-14B*, which adopt Qwen-14B as the base language model and follow the same training protocol. Finally, Express4D-MDM serves as a diffusion-based reference trained with a Motion Diffusion Model (MDM), offering a non-LLM baseline for comparison.

Semantic vs. Non-Semantic Representations. Semantic representations consistently outperform non-semantic ARKit vectors. *Base-semantic* surpasses *Base-non-semantic* across all R-Precision metrics and also demonstrates smaller distribution distances, while the gap further widens after finetuning (*Tuned-semantic* vs. *Tuned-non-semantic*). These findings highlight that explicitly exposing the meaning of each ARKit coefficient provides a more informative supervisory signal for text-motion grounding.

Table 4: Model Performance Evaluation Results Sorted by MAE

Model Configuration	Overall MSE↓	Overall MAE↓
Base-deepseek-ARKit-non-semantic	198.393021	3.345304
Base-qwen3-14b-Image-non-semantic	8.532402	2.218948
Base-qwen3-14b-original-non-semantic	7.814500	2.061756
Base-deepseek-original-non-semantic	77.067886	1.663504
Base-qwen3-14b-ARKit-non-semantic	11.099138	1.585984
Tuned-deepseek-ARKit-non-semantic	35.721793	0.904565
Tuned-deepseek-Image-non-semantic	13.330667	0.414620
Tuned-deepseek-original-non-semantic	12.071424	0.387603
Base-qwen3-4b-Image-non-semantic	0.123285	0.261439
Base-qwen3-4b-ARKit-non-semantic	0.103033	0.237061
Base-qwen3-4b-original-non-semantic	0.085073	0.213044
Base-qwen3-4b-Image-semantic	0.033737	0.093828
Base-qwen3-4b-ARKit-semantic	0.025687	0.089817
Base-qwen3-14b-Image-semantic	0.027363	0.088729
Base-deepseek-Image-semantic	0.024913	0.086483
Base-qwen3-4b-original-semantic	0.024299	0.083361
Base-deepseek-ARKit-semantic	0.023788	0.083278
Base-qwen3-14b-ARKit-semantic	0.019482	0.082952
Base-deepseek-original-semantic	0.022272	0.082861
Base-qwen3-14b-original-semantic	0.022450	0.081556
Tuned-qwen3-14b-Image-non-semantic	0.017503	0.068929
Tuned-qwen3-14b-original-non-semantic	0.017331	0.066917
Tuned-deepseek-original-semantic	0.016335	0.066142
Tuned-qwen3-14b-ARKit-non-semantic	0.016676	0.065985
Tuned-qwen3-4b-original-non-semantic	0.016216	0.065823
Tuned-deepseek-Image-semantic	0.015204	0.063333
Tuned-deepseek-ARKit-semantic	0.015578	0.060807
Tuned-qwen3-14b-original-semantic	0.013933	0.059548
Tuned-qwen3-4b-original-semantic	0.013998	0.059197
Tuned-qwen3-4b-Image-non-semantic	0.012006	0.055452
Tuned-qwen3-14b-Image-semantic	0.011411	0.053649
Tuned-qwen3-4b-Image-semantic	0.010472	0.051885
Tuned-qwen3-4b-ARKit-non-semantic	0.011215	0.051067
Tuned-qwen3-4b-ARKit-semantic	0.007245	0.039264
Tuned-qwen3-14b-ARKit-semantic	0.006906	0.038765

Diffusion Baseline. Express4D-MDM produces motions with high Diversity, consistent with the expressive sampling behavior of diffusion models. However, its significantly lower R-Precision indicates limited semantic alignment, reflecting the absence of explicit language conditioning. Moreover, its performance is comparable to the non-semantic *Vector* variants, further underscoring that motion representations lacking explicit semantic structure are fundamentally insufficient for achieving strong text–motion alignment.

Summary. Taken together, these results validate the effectiveness of interpretable ARKit semantics and LLM-based finetuning for generating high-fidelity, semantically controllable facial motion. The strong performance of *Tuned-semantic*, especially at the 14B scale, demonstrates that large language models can serve as powerful motion generators when coupled with semantically structured representations.

Table 5: Loss Comparison Across Different Configurations

Model	Data Type	Train Loss	Eval Loss
Qwen3-4B	original	0.04399845	0.05115031
	ARKit-based	0.04079014	0.04607984
	Image-based	0.04674645	0.05088831
	original-non-semantic	0.11204951	0.12501122
	ARKit-non-semantic	0.10009367	0.11942095
	Image-non-semantic	0.10147048	0.12050562
Qwen3-14B	original	0.04413972	0.05011869
	ARKit-based	0.03702557	0.04481282
	Image-based	0.04356491	0.04925121
	original-non-semantic	0.10224197	0.12059103
	ARKit-non-semantic	0.09825735	0.11423669
	Image-non-semantic	0.09463592	0.11857172
DeepSeek	original	0.04506757	0.05090072
	ARKit-based	0.03918483	0.04624721
	Image-based	0.04335775	0.04956503
	original-non-semantic	0.10576349	0.12249377
	ARKit-non-semantic	0.09627808	0.11671870
	Image-non-semantic	0.09928249	0.12036505

B Training and Implementation Details

B.1 Extensive Model Experimentation and Performance Analysis

Experimental Setup. We conducted comprehensive model performance evaluation on the KeyframeFace dataset, covering three mainstream large language models: Qwen3-14B, Qwen3-4B-Instruct-2507, and DeepSeek-R1-Distill-Qwen-14B. The experimental design employs systematic comparative analysis across three distinct annotation types—ARKit-based (enhanced annotations derived from ARKit parameters), Image-based (enhanced annotations from image analysis), and Original (original script annotations)—evaluated at both Text (semantic text format) and Vector (numerical vector format) representation levels through fine-tuning and assessment.

For clarity in result analysis and discussion, we adopted a standardized four-segment naming convention: “Training Status-Model Type-Annotation Type-Representation Format.” Specifically, the first segment identifies the model training state (“Tuned” indicating fine-tuned models, “Base” indicating pre-trained foundation models); the second segment specifies model type and scale (e.g., “qwen3-14b”, “qwen3-4b”, “deepseek”); the third segment denotes the annotation type (“ARKit”, “Image”, or “original”); the fourth segment indicates input representation format (“Text” for semantic-preserving text format, “Vector” for pure numerical vector format). For instance, “Tuned-qwen3-14b-ARKit-semantic” represents a fine-tuned Qwen3-14B model trained on ARKit-enhanced annotations using text format for infer-

ence, while “Base-deepseek-Image-non-semantic” indicates an unfine-tuned DeepSeek foundation model configured with image-enhanced annotations using vector format input.

Importantly, to ensure experimental reliability and comparability, all 36 configurations employed consistent train-test split strategies, guaranteeing fair comparisons across different models and configurations. This standardized naming approach not only ensures clear identification of experimental configurations but also facilitates systematic analysis of the specific impacts of training strategies, model architectures, data augmentation methods, and representation formats on final performance.

Results Analysis. As shown in Table 4, semantic representation plays a decisive role, with Vector format causing severe degradation in foundation models, while ARKit-based annotations consistently achieve the best performance. Only two configurations—Tuned-qwen3-14b-ARKit-semantic and Tuned-qwen3-4b-ARKit-semantic—reach breakthrough MAE levels around 0.039, demonstrating the effectiveness of combining ARKit annotations with text input. Although larger models generally perform better, several 4B configurations exceed certain 14B counterparts, indicating non-linear scale effects and possible overfitting in larger models, which is further supported by the training and validation loss trends in Table 5.

B.2 Prompt Engineering and Training Framework

To implement the text-to-ARKit generation functionality described in our methodology, we developed a structured training data generation framework. This framework employs a three-tier prompt structure based on prompt engineering: System Prompt (P_{sys}), Script (S), and Target Frame Instruction (I_{key}).

The Script S contains background information, emotional descriptions, and detailed keyframe description sequences, providing rich contextual information for the recursive keyframe generation strategy in our algorithm. The Target Frame Instruction I_{key} generates corresponding task instructions for each specific keyframe after extracting keyframe boundaries through the $f_{\text{key}}(S)$ function, guiding the model to generate corresponding ARKit parameters. This structured design fully leverages the linguistic prior knowledge of LLMs, enabling the model to understand complex facial expression semantic descriptions and precisely map them to the 61-dimensional ARKit coefficients, achieving effective conversion from natural language descriptions to facial animation parameters.

B.3 Semantic vs. Non-Semantic Representation Training Format

To thoroughly investigate the role of semantic information in facial parameter learning, we designed two distinct training formats. The semantic format P_{sem} contains the complete System Prompt P_{sys} , Target Frame Instruction I_{key} , and Script S , providing detailed parameter explanations and semantic mappings; while the non-semantic format $P_{\text{non-sem}}$ completely removes System Prompt P_{sys} , containing only Target Frame Instruction I_{key} and Script S , without providing any semantic hints related to the coefficients.

The semantic format preserves complete semantic guidance from the system prompt and structured JSON output, maintaining parameter names and semantic structure. In contrast, the non-semantic format completely omits the system prompt, eliminating all linguistic cues and semantic information about ARKit parameter meanings.

This contrastive design supports the four experimental configurations in our semantic understanding evaluation: Base-non-semantic, Base-semantic, Tuned-non-semantic, and Tuned-semantic. By completely eliminating semantic cues, we can precisely isolate and measure the contribution of semantic information to ARKit parameter generation, validating the importance of LLMs’ linguistic priors in facial expression parameter learning. This design enables us to quantitatively analyze the specific role of semantic information in improving parameter generation accuracy and expression consistency.

C Evaluation Model Details

C.1 R-Precision

R-Precision is used to evaluate retrieval performance by examining whether the ground-truth motion corresponding to a given text description appears within the top- $K(3)$ ranked candidates. For a batch of size $N(32)$, we compute a cosine-similarity matrix $S_{ij} = \text{sim}(\mathcal{T}_i, A_j)$ and determine the rank of the matched motion A_i for each query \mathcal{T}_i . R-Precision@K is then defined as

$$\text{R-Precision@K} = \frac{1}{N} \sum_{i=1}^N \mathbf{1}[\text{rank}(A_i|\mathcal{T}_i) \leq K],$$

indicating the proportion of queries whose correct matches fall within the top- K . Higher values reflect stronger cross-modal discriminative ability.

C.2 Multimodal Distance (MMD)

Multimodal Distance measures the geometric proximity between matched text and motion embeddings in the learned joint space. For each sample pair (\mathcal{T}_i, A_i) , we compute the

Euclidean distance between their normalized embeddings and take the average over all pairs:

$$\text{MMD} = \frac{1}{N} \sum_{i=1}^N \|f_{\text{text}}(\mathcal{T}_i) - f_{\text{motion}}(A_i)\|_2.$$

Lower values indicate that the text and motion embeddings are located closer together, suggesting stronger semantic alignment.

C.3 Evaluation Model Training Details

The evaluation model is trained end-to-end using a symmetric InfoNCE loss, which encourages matched text–motion pairs to have high similarity while pushing unmatched samples apart. The loss is defined as

$$\mathcal{L} = \frac{1}{2}(\mathcal{L}_{\mathcal{T} \rightarrow A} + \mathcal{L}_{A \rightarrow \mathcal{T}}),$$

with a temperature parameter $\tau = 0.07$, and is applied over all text–motion pairs within each batch. Training employs the AdamW optimizer with a learning rate of 1×10^{-4} and weight decay of the same magnitude, together with a cosine-annealing learning-rate schedule. We train the model for up to 1000 epochs and apply early stopping when the R-Precision@1 on the validation split does not improve for ten consecutive epochs. Both the text encoder and motion encoder are fully trainable during optimization. Motion features are standardized using Z-score statistics computed from the training set, while text descriptions are tokenized with the MiniLM/BERT tokenizer. A fixed random seed (42) is used throughout to ensure reproducibility of the results.

D KeyframeFace Dataset Analysis

D.1 Data Collection and Actor Composition

We recruited 21 professional actors (anonymized as A01–A21), including 8 male and 13 female performers. To achieve natural and authentic performances, we adopted a flexible performance guidance strategy: we first used ChatGPT to generate initial scripts based on specific instructions as a performance framework. However, considering that automatically generated scripts might contain unreasonable or uncoordinated elements, we encouraged actors to incorporate their own understanding and cognition based on specific background settings and target emotions during performance, allowing them to appropriately modify script content to achieve the most natural and reasonable emotional expression effects. This human-machine collaborative creation approach ensures both data diversity and performance authenticity and appeal. After recording completion, we precisely aligned the raw facial motion data with timestamps, extracted the most expressive segments, and paired each segment with

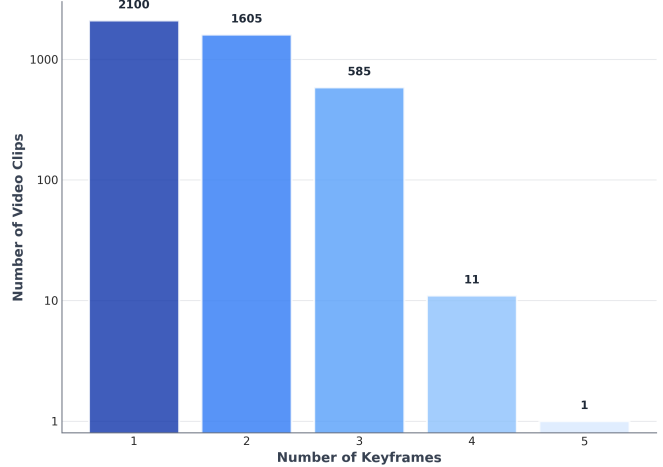


Figure 8: **Distribution of Keyframes per Video Clip.** The dataset exhibits a reasonable keyframe distribution pattern with most clips containing 1-3 keyframes, reflecting typical emotional expression structures.

corresponding text descriptions and concise emotional intent labels.

D.2 Keyframe Extraction and Distribution Characteristics

In facial expression analysis, the number of keyframes directly affects the granularity of emotional expression and model training effectiveness. As shown in Figure 8, our dataset exhibits a reasonable keyframe distribution pattern: all 2,100 video clips contain at least one keyframe, with 76.4% of clips (1,605) containing two keyframes, 27.9% of clips (585) containing three keyframes, while clips containing four or five keyframes are relatively rare (11 and 1 respectively). This distribution reflects that most emotional expression clips have clear onset-climax or onset-development-climax structural patterns, while a few complex clips exhibit richer multi-stage emotional changes. Notably, since our method focuses on generating ARKit parameters for individual keyframes based on text descriptions, the model actually learns the mapping relationship from text semantics to facial expressions at specific moments, rather than relying on sequence length-dependent temporal modeling. This design philosophy gives our method unique advantages: even under the training distribution dominated by 1-3 frames, the model can effectively generalize to complex emotional expression tasks containing more keyframes, demonstrating excellent cross-sequence-length generalization capability. This natural distribution of keyframe numbers not only reflects the characteristics of real emotional expressions but also provides ideal experimental conditions for validating the generalization and robustness of our method.

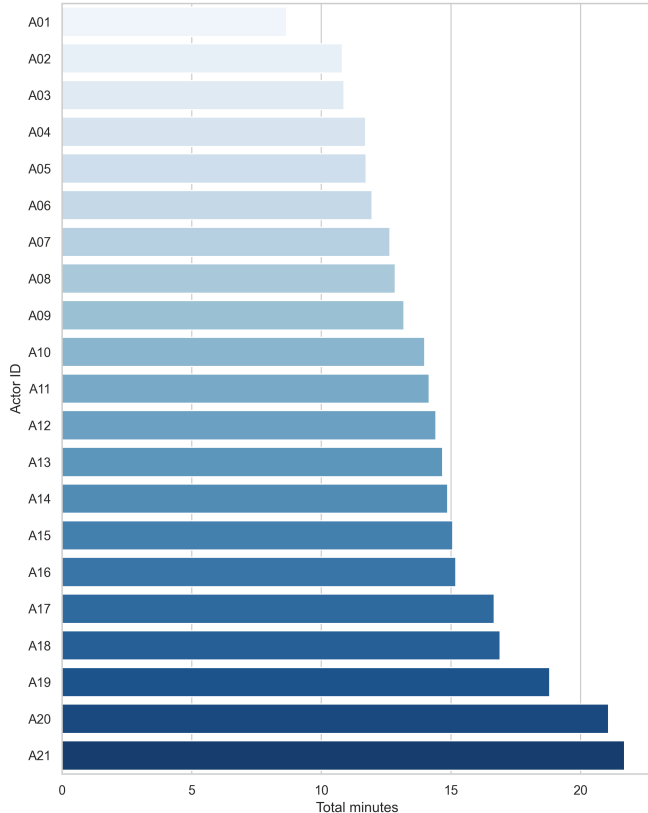


Figure 9: **Recording Duration per Actor.** Distribution of total recording minutes across all 21 anonymized actors (A01–A21), showing variation in individual contribution while maintaining balanced clip counts.

D.3 Data Distribution and Balance

As shown in Figure 9, each actor contributed a roughly balanced number of clips (100 clips per actor), though total recording durations vary somewhat. This design intentionally preserves the individualized characteristics of different actors, including unique facial structures, performance habits, and emotional expression styles, providing diverse training samples for model learning.

D.4 Clip Duration Characteristics

The video clip duration distribution in our dataset is reasonable and practical. As shown in Figure 10, clip durations range from 1.9 to 21.3 seconds with a median of 8.3 seconds. Short clips mainly capture instantaneous emotional reactions (such as surprise, fear), while long clips contain complete emotional development and change processes. Notably, 75% of clips are concentrated within the relatively narrow range of 6.6-10.3 seconds, and this consistency greatly simplifies batch processing operations and frame sequence sampling strategies during model training.

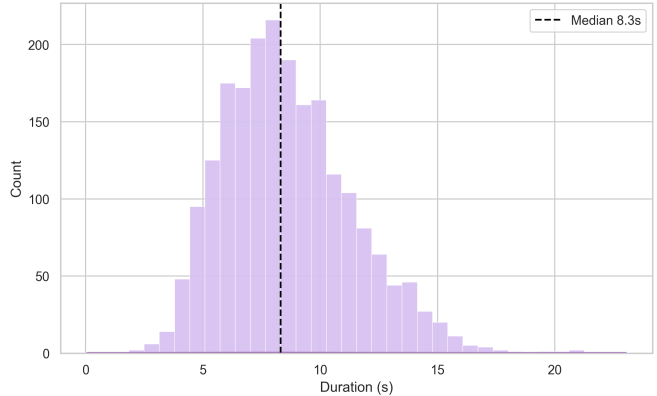


Figure 10: **Video Clip Duration Distribution.** Histogram showing the distribution of clip durations across the dataset, with median duration of 8.3 seconds.

D.5 Frame-level Emotion Analysis

To comprehensively characterize the emotional dynamics within our dataset, we conduct fine-grained emotion analysis at the keyframe level. Since character emotions evolve with narrative development in scripts, single video-level labels are insufficient to capture this dynamic variation. Therefore, we extract keyframes from each video and employ the Qwen3-30B model for quantitative emotion assessment.

Following Ekman’s emotion theory framework, we define six basic emotion categories: Sadness, Surprise, Anger, Happiness, Disgust, and Fear. For each keyframe, the model comprehensively analyzes ARKit facial expression parameters (52 blendshape parameters and 9 head pose parameters), script contextual descriptions, and emotional context to generate intensity scores ranging from 0 to 1 for each of the six emotions, ultimately outputting structured JSON-formatted emotion parameters. This keyframe-based multimodal analysis approach enables precise capture of subtle emotional expressions that vary over time in facial animations.

As shown in Figure 11(b), the dataset is dominated by sadness (37.7%) and happiness (36.8%), which together comprise nearly 75% of keyframes, reflecting typical dramatic emotional contrast. The remaining emotions—surprise (7.9%), anger (7.7%), fear (7.3%), and disgust (2.6%)—appear less frequently but are essential for representing a full emotional spectrum.

Figure 11(a) visualizes the t-SNE projection of six-dimensional emotion vectors. Distinct clusters—for example, happiness and sadness—indicate clear emotional extremes, while smooth color transitions reveal abundant mixed and intermediate emotions. This demonstrates that the dataset spans both pure and composite emotional states.

In summary, our dataset demonstrates broad coverage and realistic distribution characteristics across three dimensions: emotion categories, intensity ranges, and emotion combina-

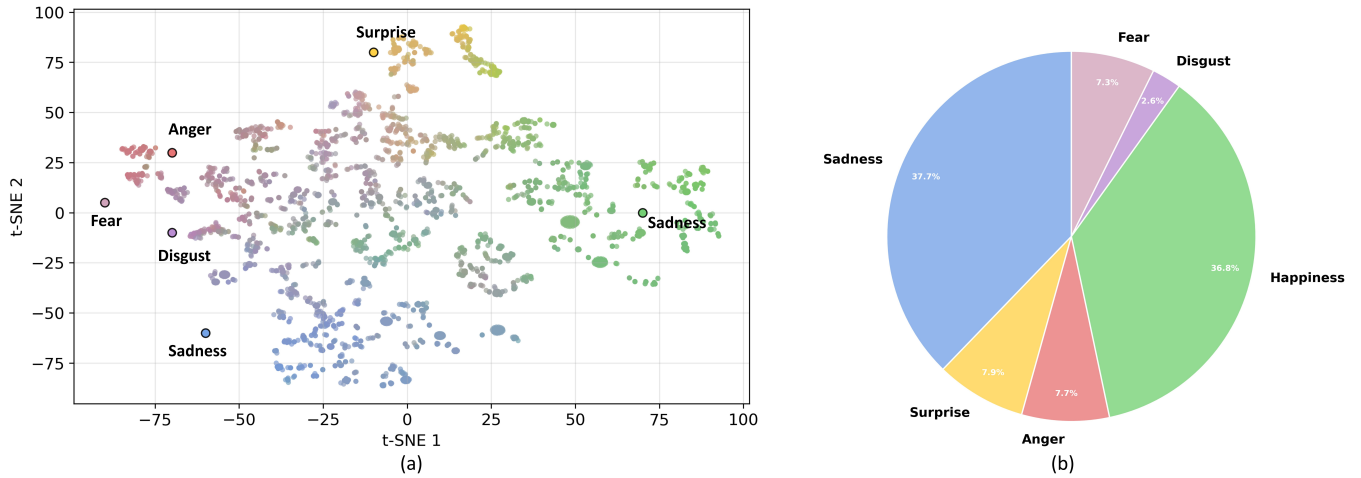


Figure 11: **Emotion Distribution and Visualization.** (a) t-SNE projection of keyframes colored by emotion intensities. (b) Distribution of dominant emotions across all keyframes.

tions. This provides high-quality, diverse training data for downstream tasks such as facial expression generation and emotion recognition, offering significant research value and application potential.